Graphical Abstract

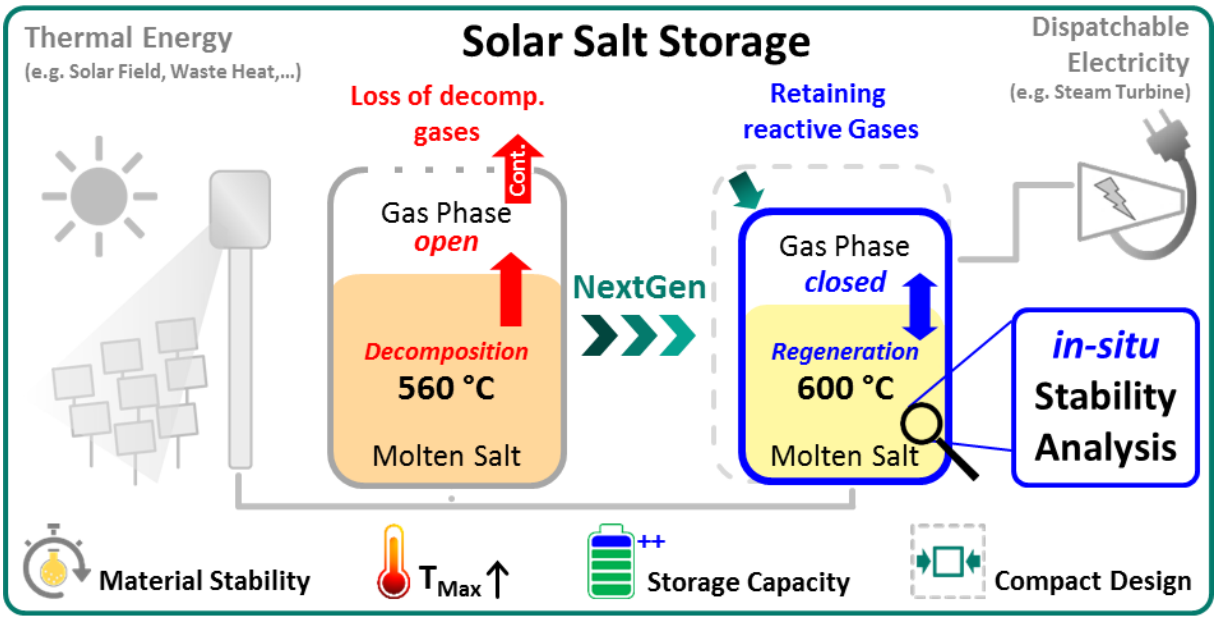

Highlights

Thermal stability limit of molten nitrate salts is enhanced from 560 °C to 600 °C

Operation in a closed storage system increases thermal stability significantly

Performance of Solar Salt is demonstrated in 100 g-scale

Quasi-in situ sample analysis is used for proof of concept

Formation of corrosive impurities is successfully suppressed at 600 °C

Solar Salt - pushing an old material for energy storage to a new limit

Alexander Bonk a,* Markus Braun[a], Veronika A. Sötz[b], Thomas Bauer[b]

[a] German Aerospace Center (DLR), Institute of Engineering Thermodynamics, 70569 Stuttgart, Germany

[b] German Aerospace Center (DLR), Institute of Engineering Thermodynamics, 51147 Köln, Germany

* Corresponding author

Email address. alexander.bonk@dlr.de

Abstract

The implementation of inexpensive and reliable energy storage technologies is crucial for the decarbonisation of energy intensive industry branches and energy supply. Sensible thermal energy storage (TES) in molten salts is a key technology for storage of heat in the scale of gigawatt hours but currently limited to operating temperatures of 560°C. Increasing the maximum operating temperature while maintaining thermal stability of the storage medium is one of the main challenges next-Generation TES systems are facing. Extending the upper temperature limit by only 40 °C increases the storage capacity by more than 16 % allowing for more compact storage designs and cost savings in the $ million-range for large scale storage units. Here we propose a novel storage technology from a materials point of view that pushes the thermal stability limit of Solar Salt up to 600 °C by simply but effectively sealing the storage unit including the gas system. The concentration of the unstable nitrite ion and of the corrosive oxide ion could be reduced by 16 % and 75 %, respectively at 600 °C, compared to a salt system with open atmosphere. We present clear evidence of the enhanced thermal stability in long-term, 100 g-scale test campaigns at previously unequalled temperatures. These findings constitute a major advance in the design and engineering of next generation storage systems.

Keywords. Thermal Energy Storage, Molten Nitrate Salt, Enhancing Thermal Stability, Solar Salt

1. Introduction

The dispatchability and efficiency of modern concentrating solar tower plants relies on the use of stable high temperature storage and heat transfer media.[1-3] Molten nitrate salts, in particular Solar Salt (60 % $NaNO_3$ - 40 % KNO_3 by weight), are established state-of-the art storage and heat transfer materials that currently allow for operation temperatures up to around 560 °C. This upper temperature limit is set to minimize decomposition reactions that affect the thermal properties as well as corrosion towards container materials and this limit has been investigated extensively in the last decades.[4-7] It is an established goal to reach higher operating temperatures to increase the solar-to-electricity efficiency of the CSP plant and at the same time increase the volumetric storage capacity which is related to the applicable ΔT.[8, 9] The use of novel molten salt candidates for temperatures above 560 °C, such as chloride salts, is still limited by extreme constraints regarding corrosion and is therefore far from industrial implementation.[10] Conventional nitrate salts could in turn still be used at higher temperatures if the chemical equilibria of the decomposition reactions are systematically shifted to the reagent side. We will present clear evidence that the latter option is viable even at an advanced lab-scale. To understand the concept one has to assess the decomposition mechanism of nitrate salts at high temperatures, which is complex but can be broken down to a few accepted reactions. The nitrate ion (NO_3^-) tends to be in equilibrium with atmospheric oxygen to form nitrite (NO_2^-) according to Eq. 1.[11, 12]

$$\boldsymbol{NO_3^- \rightleftharpoons NO_2^- + \frac{1}{2} O_2} \qquad 1$$

Eq. 1 can be observed at every scale (lab or large-scale tank) and temperature.[5, 12, 13] For Solar Salt the nitrate content at 560 °C at P_{O_2} = 0.2 atm is typically around 95 mol%, while the nitrite content is close to 5 mol%.[7] Experimental methods to determine a nitrate salts thermal stability limit and authors of this work and a thorough review will therefore not be provided here.[14] As a summary, there is consensus that a defined nitrate-nitrite equilibrium is established at 560 °C in air with around 95 mol% NO_3^- and 5 mol% NO_2^-. Nissen and Meeker [5] demonstrated, that by increasing the P_{O_2} the equilibrium of reaction 1 can be shifted to the nitrate side substantially, resulting in significantly lower nitrite concentrations at the same temperature. Thermodynamic data on oxide ion formation is hardly available due to

the fact that first, the stoichiometry of the oxide forming reaction and gaseous by-products remain unclear and might depend on the applied temperature, and second, experimental methods are extremely sensitive to correct handling of the molten salt. The nitrite ion itself is also not a stable species but can decompose and several reaction mechanisms have been published. All of them propose the formation of oxide ions along with different gaseous species such as nitrous gases (NO, NO_2, etc.), oxygen, or nitrogen.[15-18] One of the reactions is that shown in Eq. 2.

$$\boldsymbol{NO_2^- \rightleftharpoons O^{2-} + NO + NO_2} \qquad 2$$

where the nitrite ion forms an oxide ion (more easily understood as Na_2O or K_2O in a chemical sense) that is dissolved in the melt, and different nitrous gases (whose complex high temperature chemistry will not be explained at length).[7] The oxide ions formed by Eq. 2 can increase the basicity of the molten salt and are suspected to enhance corrosion effects towards metallic alloys (e.g. containers, pipes, valves, pumps) [4, 19-21]. Dorcheh et al. demonstrated that chromium ferritic steels cannot be considered corrosion resistant in Solar Salt at 600 °C, but that SS316 and SS347H exhibit slow parabolic corrosion kinetics, proving their protective behavior.[22] Bradshaw et al. identified rapidly increasing corrosion rates above 600 °C for different steel types with Alloy 800 being more resistant than SS316. Bradshaw also stated that peroxides are considered stable above 600 °C and that their presence certainly exacerbates corrosion above 615 °C.

After all, by the chemical nature of both salt decomposition reactions the most feasible way of shifting the equilibrium towards the reagent side, would be an increase of the partial pressures of O_2 and NO_x gases. Hypothetically, this could be achieved by flushing storage tanks with synthetic gas atmospheres containing unusually high O_2 and NO_x contents, or by hermetically sealing the system. The latter would prevent the loss of product gases formed during decomposition and may effectively shift the chemical equilibrium to the nitrate-side. This in turn reduces the concentration of oxide ion impurities which, as demonstrated in one of our previous publications, affects corrosion resistance of some steels significantly.[23]

Systematic studies on nitrate salt chemistry in a closed system in the 100 g to 200 g scale have not been performed to our best knowledge especially since *in-situ* extraction of molten salt was not possible up to now. In this study, by the use of an advanced isothermal test rig combined with an in-house engineered autosampler, we

present the first set of experiments where Solar Salt is stored in, what is hereafter referred to as, a *closed* system in terms of molten salt and gas atmosphere. The experiments feature unique *in-situ* sample extraction as well as pressure and temperature control. We present clear experimental evidence that transition from commonly used *open*- to a *closed* storage system pushes the thermal stability of Solar Salt to new limits. To obtain thermodynamic equilibrium data for comparison, a large series of experiments is conducted in classical open systems at temperatures between 500 °C and 600 °C and at different P_{O_2}. Experiments in closed systems are performed at different temperatures up to 600 °C and feature automated *in-situ* sample extraction. Due to this novel extraction method for closed systems it is possible for the first time to correlate pressure build-up and changes in the molten salt chemistry in a closed system *quasi in-situ*. When all gaseous reaction species are retained within the setup the nitrite and oxide ion formation can be suppressed substantially and higher operating temperatures become possible.

2. Methods

Solar Salt was produced by mixing $NaNO_3$ (> 99 %, Merck, Germany) and KNO_3 (>99 %, Merck, Germany). Isothermal storage was performed in an in-house engineered isothermal autoclave test rig, described in one of our earlier studies [24]. In summary, the salt precursors are mixed in a tubular alumina crucible with around 180 mm height, which is placed in a tubular stainless steel chamber that is sealed with a flange containing inlets for thermocouples, a stirrer, as well as means for sample extraction (Figure 1). The top of the stainless steel chamber is passively cooled with pressurized air, to minimize molten salt creeping out of the crucible.

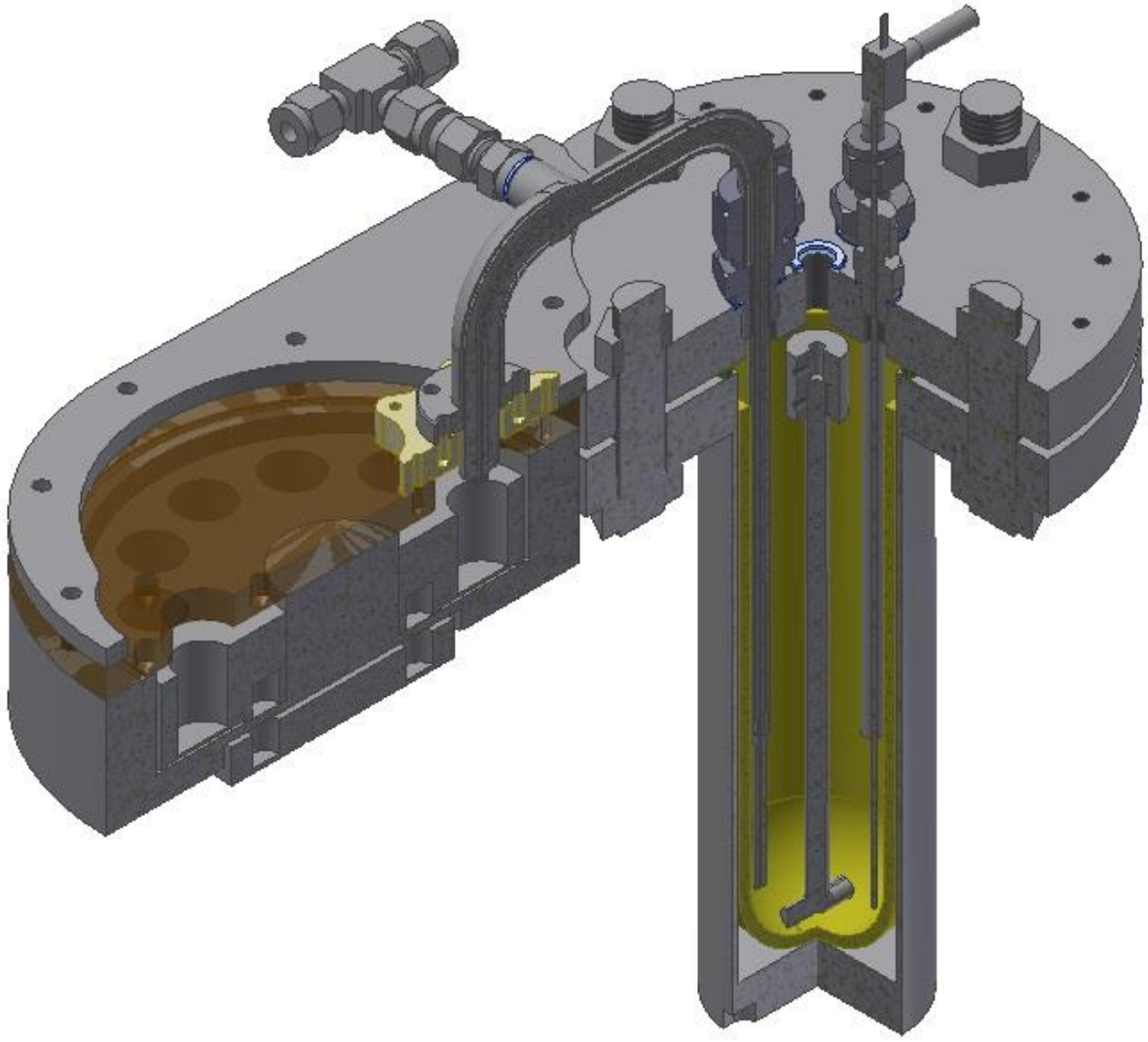

Figure 1 Schematic of the storage system and autosampler used for the storage of Solar Salt in a closed configuration.

For experiments performed in an open configuration a constant gas flow was purged on top of the molten salt. Sample extraction was performed using a stainless steel tube as a type of pipette. For experiments in a closed configuration the molten salt is

heated to 300 °C for dehydration, followed by a leakage test where the system is sealed and pressurized with synthetic air up to 1 bar overpressure and the pressure is then recorded as a function of time. Afterwards the gas system is evacuated, purged with synthetic air (5.0 grade, 100 mL min^{-1} and the molten salt is heated to the desired temperature of the experiment (550 °C, 580 °C or 600 °C). Subsequently, when this temperature is reached the gas flow is stopped and the gas system is immediately sealed. For experiments in the closed configuration sample extraction was automated with an in-house engineered autosampler which is shown schematically in Figure 1 and will be described in the supplementary part of this work in more depth. Most importantly, the gas systems of the autosampler and the crucible are connected and the whole system is hermetically sealed during the experiments to retain product gases on top of the melt. Sample extraction is carried out with a riser tube made of Inconel (see more detailed description in Supplementary Material) by applying an underpressure in the autosampler cell thereby forcing molten salt to flow from the crucible into the sampling cylinders. The total volume of the (empty) autoclave test rig including the autosampler was determined to be 677 mL using a water displacement method and the volume of the molten salt during the experiments was derived from its weighed portion and temperature dependent density data.[25] The derived volumes were used for ideal gas calculations in different parts of this work. Oxide ion concentrations were analyzed using potentiometric acid-base titration (Metrohm Titrando 905) with 0.01 m to 0.1 m HCl solutions, produced from Titrisol® -standard solutions, automatically dosed using Metrohm 800 Dosino units. Oxide ions are transformed into hydroxide ions when the salt sample is dissolved in water. Equivalence points were used to determine hydroxide ions using the Warder method for data analysis.[26]

3. Results and Discussion

3.1. Molten salt chemistry up to 560 °C in open configuration

The storage of Solar Salt at around 560 °C sets the benchmark in terms of thermal stability for different nitrate salt systems in the CSP-TES sector.[27] To establish a set of equilibrium data under relevant conditions, Solar Salt has been subjected to different temperatures and P_{O_2} and samples have successively been extracted and analyzed in terms of the ion fractions of. NO_3^-, NO_2^-, and O^{2-}. The molar ion fractions

have been calculated assuming that the mentioned anions represent the main (anion-) fraction of the molten salt.

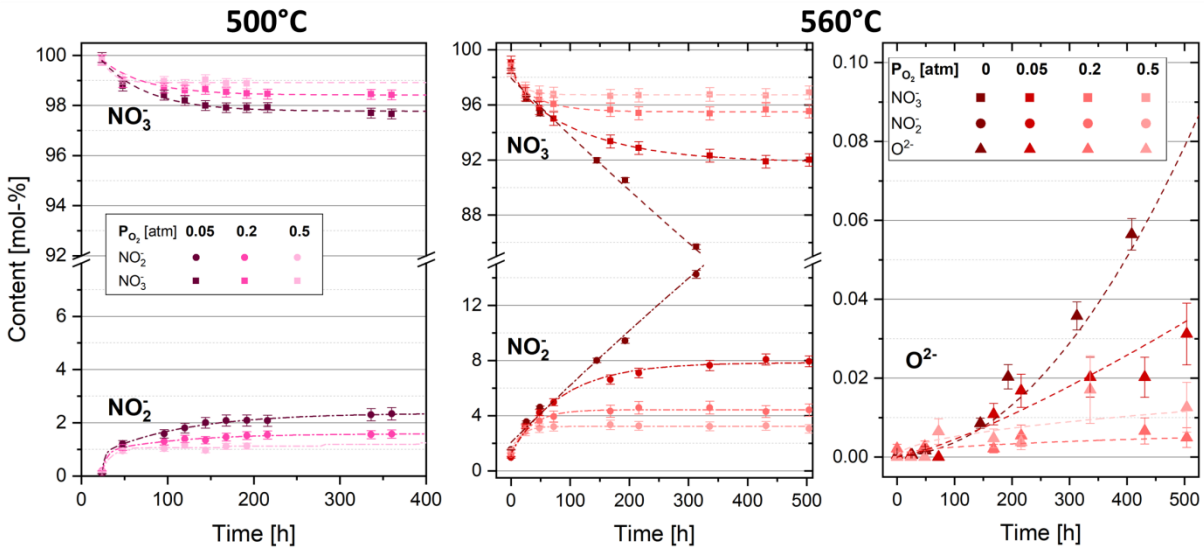

Figure 2 Molar nitrate and nitrite content in Solar Salt stored at (a) 500 ◦C, (b) 560 °C as well as (c) contents of oxides at 560 °C at different P_{O_2} (0, 0.05, 0.2 or 0.5 atm) as shown in the legend of the respective figures. The legend in (c) also holds true for the symbols used in (b). The presented fits serve as guide to the eye.

The first set of data under different P_{O_2} and under N_2-gas is shown in Figure 2. The provided data set in *open* configuration is ultimately required to compare it with the molten salt chemistry in *closed* configuration, which is shown in a later chapter.

As shown in Figure 2(a), at 500 °C the nitrate levels in a Solar Salt sample, when in steady-state, are 97.5 mol% / 98.4 mol% / 98.9 mol% at 0.05 / 0.2 / 0.5 atm O_2 in N_2. The remaining anion fractions in the molten salts were identified as nitrites, while no oxides or other anionic species were detected by ion chromatography and titration. At 560 °C the nitrate contents in Solar Salt are overall lower compared to 500 °C, since the chemical equilibrium of reaction 1 shifts to the nitrite side. At P_{O_2} of 0.05 / 0.2 / 0.5 atm equilibrium values of nitrate are 92 mol%, 95.5 mol% and 96.9 mol%, respectively. The values at both 500 and 560 °C are in agreement with previously published thermodynamic data.[5, 14, 28] Therefore, it is reasonable to interpret the salt composition towards the end of the experiments as equilibrium composition with regard to the nitrate and nitrite content. Also, it becomes obvious that the applied experimental method is suitable for comparisons with other equilibrium studies. Over the course of the experiment traces of oxides can be detected (Figure 2(c)), but the maximum value is below 0.05 mol% for P_{O_2} > 0.05 atm and can therefore be considered negligible. Equilibrium is typically reached within the first 200 h of all

experiments. Yet, time for equilibration appears to increase with decreasing temperature and decreasing P_{O_2} with the quickest equilibration measured at 560 °C and P_{O_2} = 0.5 atm. Under N_2 atmospheres no nitrate-nitrite equilibrium is established. The NO_3^- levels decrease-, while the NO_2^- levels increase steadily which is indicative of ongoing decomposition over the course of the measurement. Although the rate of decomposition seems to decline over the duration of the experiment, no equilibration is observed. Furthermore, the decomposition of the nitrite ion to form oxide ion species can be verified. It is reflected by the steadily increasing oxide ion content shown in Figure 2(c). The drastic change of molten salt composition under N_2 gives rise to severe changes of the molten salts thermo-physical properties but may also affect corrosiveness of the molten salts, since oxides are assumed to aggravate corrosion, as mentioned earlier.

3.2. Molten salt chemistry at T>560 °C in open configuration

The anion composition of Solar Salt exposed to temperatures between 500 °C and 600 °C over time is shown in Figure 3, wherein the data at 500 °C and 560 °C is identical to the one shown in (Figure 2). At 580 °C the nitrate content in Solar Salt decreases as compared to 500 °C and 560 °C with increasing nitrite content and higher oxide contents as compared to the lower temperatures. In steady state the nitrate and nitrite contents are 94.5 mol% and 5.5 mol%, respectively.

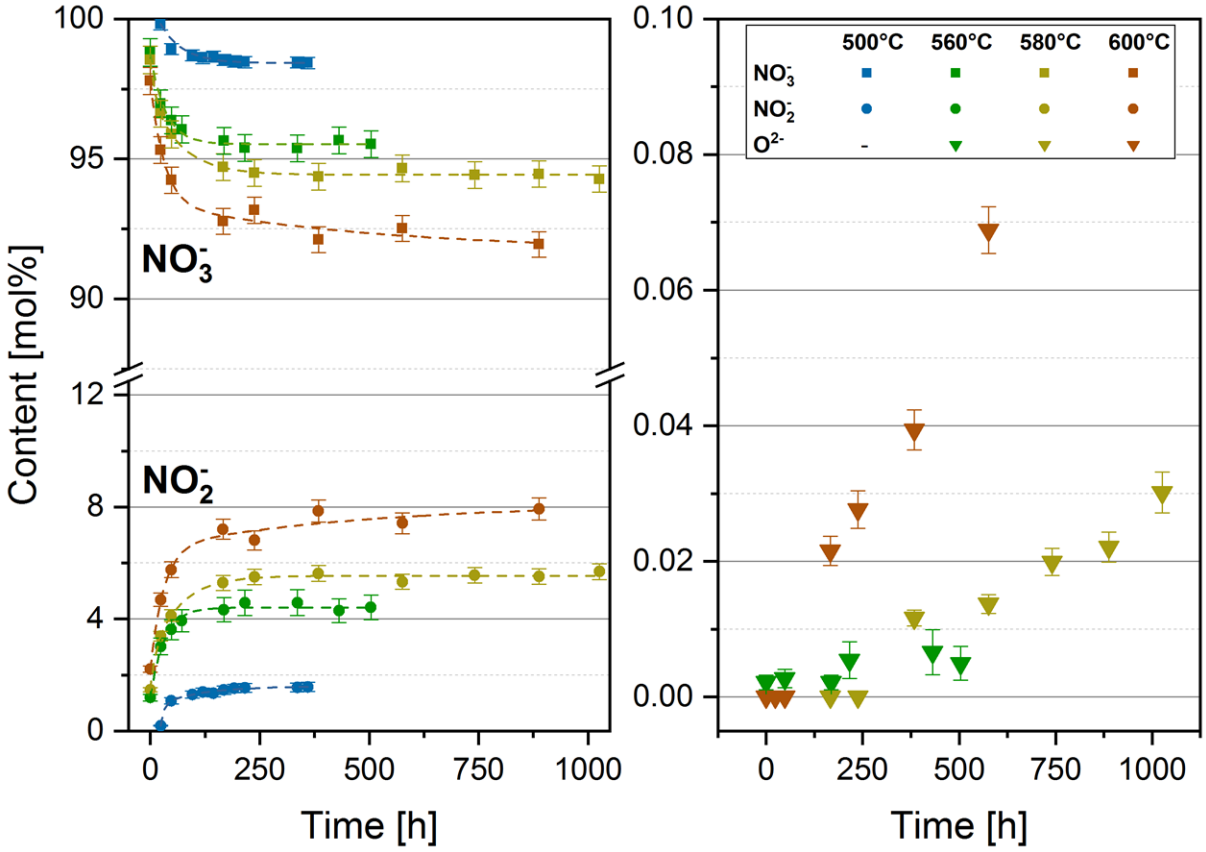

Figure 3 Molten Salt composition in Solar Salt stored at 500 °C, 560 °C, 580 °C and 600 °C purged with a gas containing 0.2 atm O_2 in N_2.Fits serve as guide to the eye

Compared to experiments performed at 560 °C the oxide content increases steadily and at a higher rate at 580 °C, with final values of 0.03 mol%. The equilibrium of reaction 2 is however not reached after 1000 h. The reason is clearly the constant removal of the nitrous gases formed during the decomposition reactions. At 600 °C the nitrate content is the lowest, and the nitrite content is the highest of all temperatures evaluated. A nitrate-nitrite equilibrium can be established at around 92 mol% (64.5 wt%) nitrate and 8 mol% (4.4 wt%) nitrite. The nitrite concentration is slightly lower but yet in good agreement with thermodynamic data from Nissen *et al.*, who propose a nitrite content of 5.19 wt% at 600 °C at a P_{O_2} of 0.2 atm, but in an equimolar $NaNO_3$-KNO_3 melt.[5] The oxide levels increase at a higher rate as compared to the other experiments, indicating accelerated decomposition of the molten salt. Overall the results indicate that there is a limit in operation temperature for Solar Salt. Nonetheless, we have to clarify that this maximum operating temperature can hardly be broken down to a single temperature. It rather presents a trade-of between acceptable levels of nitrite formation, which affect the thermal properties of the salt, and even more so the rate of oxide ion formation. The latter

can directly be correlated with the corrosivity of the melt, and thus the long-term stability of container materials and furthermore, constant emission of toxic nitrous gases must be taken into account in an industrial scale.

3.3. Molten Salt chemistry at T>560 °C in closed configuration

This chapter presents the highly novel experimental results of nitrate salt salts isothermally stored under closed atmosphere. For the first time, those experiments could be performed, and their significance becomes even more meaningful given they are comparable with the data presented, under a purged gas atmosphere in chapter 3.2.

Chronologically, the first set of experiments in what is referred to as a closed system, was performed before the build-up of the autosampler, thus molten salt samples were only extracted immediately after finishing the experiment. Figure 4 shows one of the first isothermal storage experiments in a closed system. Solar Salt was heated to 150 °C for dehydration, pre-melted and a leakage test was carried out at 300 °C. From there on, the molten salt was heated to 550 °C and after reaching this temperature the molten salt and gas phase were sealed immediately. The pressure sensors show an immediate increase in (over)pressure, which seems to equilibrate after 50 h at around 0.85 bar, but then steadily decreases until the end of the experiment to around 0.77 bar. The pressure loss towards the end of the experiment (between 100 h and the end of the experiment) can be explained by gas leaking which was confirmed by blank experiments. It is important to highlight, that fluctuations in pressure can be observed which could be traced back to the fact that a relative pressure sensor was used for monitoring. This sensor therefore effectively recorded changes in atmospheric pressure in the laboratory, which could be confirmed by comparing the live experiment with atmospheric data available (data correction was not performed for clarity). The molten salt chemistry after the experiment was investigated yielding a nitrite content of 2.5 mol% and a nitrate content of 97.4 mol%, with only minor oxide ion quantities of 0.01 mol%. The nitrite content is measurably lower as compared to the experiment in an open atmosphere at 550 °C (4.5 mol%), indicating the equilibrium of reaction 1 has been shifted to the nitrate side significantly.

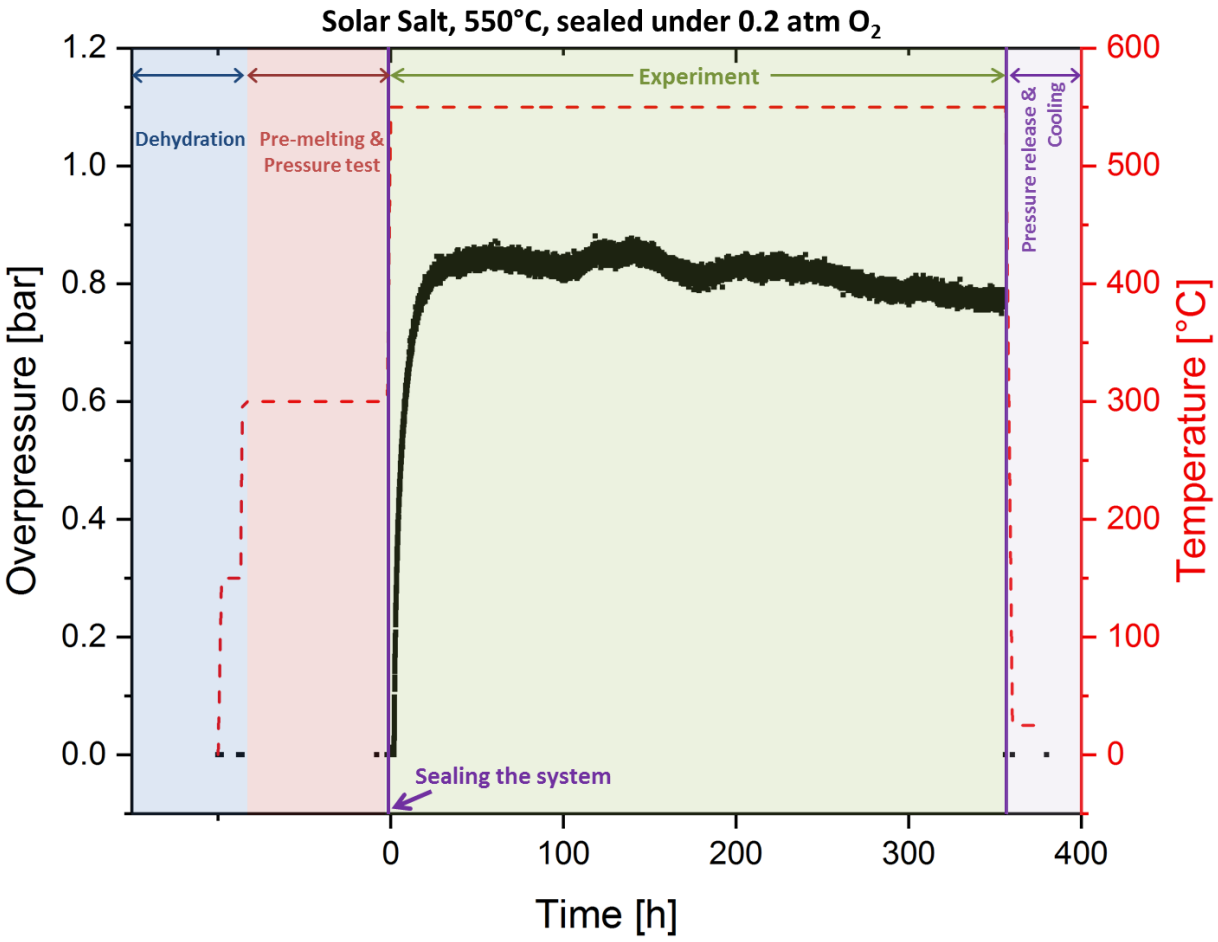

Figure 4 Experimental heating procedure and pressure data for a long-term isothermal test of Solar Salt in a closed system. The salt was dehydrated and pre-melted under synthetic air and heated to 550 °C, where the salt and gas system were sealed and the pressure increase was recorded. After 360 h the experiment was stopped by cooling the salt and releasing the pressure.

3.4. Experiments in closed systems with in-situ sample extraction

The autoclave test rig was eventually complemented with the in-house engineered autosampler and experiments at 550 °C with Solar Salt in a closed system were repeated but using in-situ sample extraction. Figure 5 shows the pressure data of an experiment comprising 150 g Solar Salt in the closed system and the molten salt chemistry of 11 samples extracted in-situ after 0, 2, 4, 6, 10, 20, 50, 100, 200, 300 and 354 h.

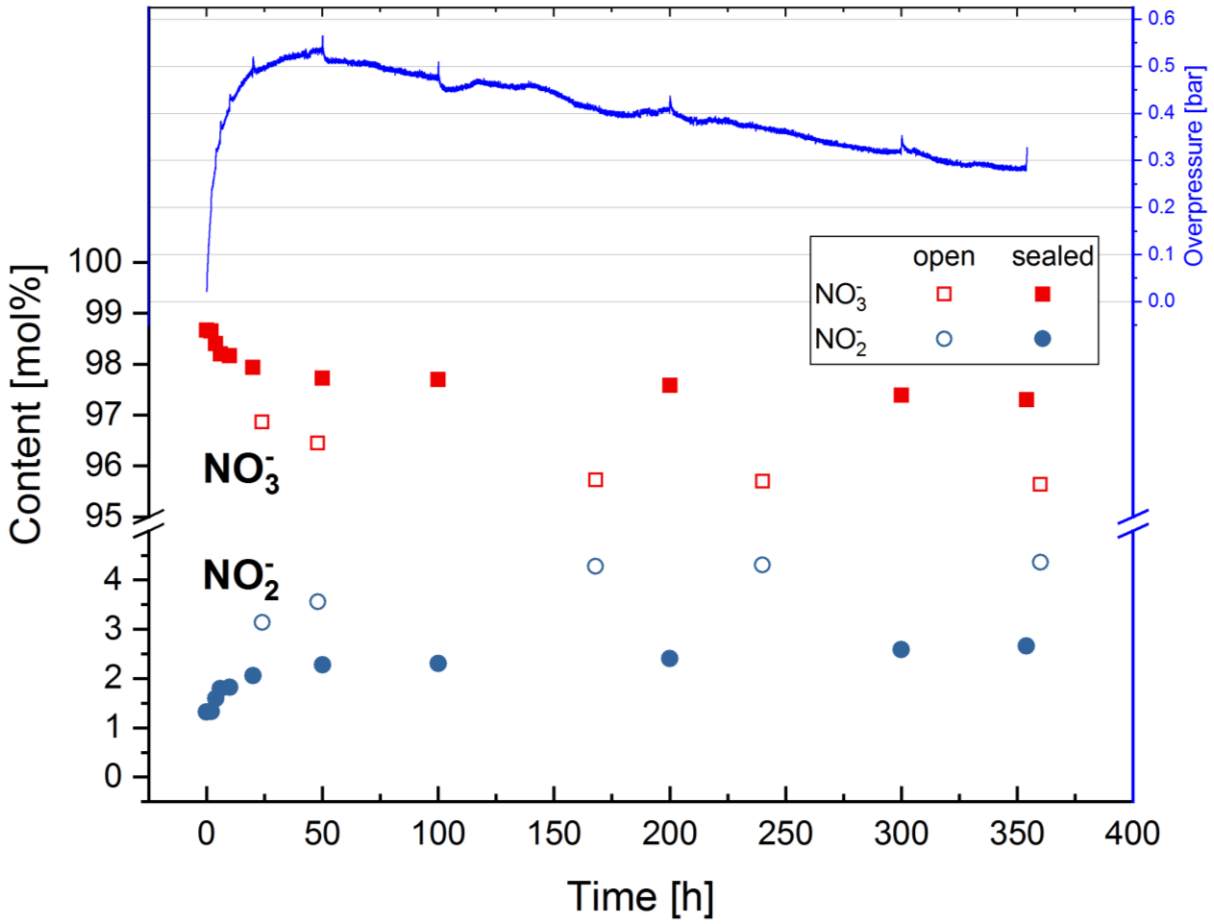

Figure 5 Pressure build-up and nitrate/nitrite chemistry in Solar Salt stored at 550 °C. In the *open* system the salt was purged with an atmosphere of 0.2 atm O_2 in N_2. In the *closed* system the salt was purged with the same gas during heating until the intended salt temperature was reached (550 ◦C) and then the system was sealed in terms of salt and gas atmosphere.

The first observation is that the pressure behaves very similar to the experiment shown in Figure 4 although the maximum pressure is slightly lower. Over the duration of the experiment a certain leakage is observed and individual sampling steps result in a small pressure peak, which is due to the mechanical procedure applied for sample extraction. The starting molar nitrite content (at t = 0h) is 1.33 mol% but further increases until it reaches equilibrium after 50 h at 2.5 mol%. The formation of a chemical equilibrium of reaction (1) could be assumed due to the steady state of the nitrate and nitrite concentrations from 50 h onwards. These concentrations in the closed system are considerably lower than the equilibrium values found in the open configuration (Figure 5). No significant amount of oxide ion species is detected over the whole duration of the experiment indicating that equilibrium reaction 2 is shifted to the nitrite side. The results also validate that the changes in the nitrite-nitrate chemistry directly correlated with the increment of pressure. More precisely, the pressure stabilizes alongside the nitrite and nitrate contents, which demonstrates that

the main contribution of pressure increment can be attributed to the evolution of gaseous oxygen at this temperature.

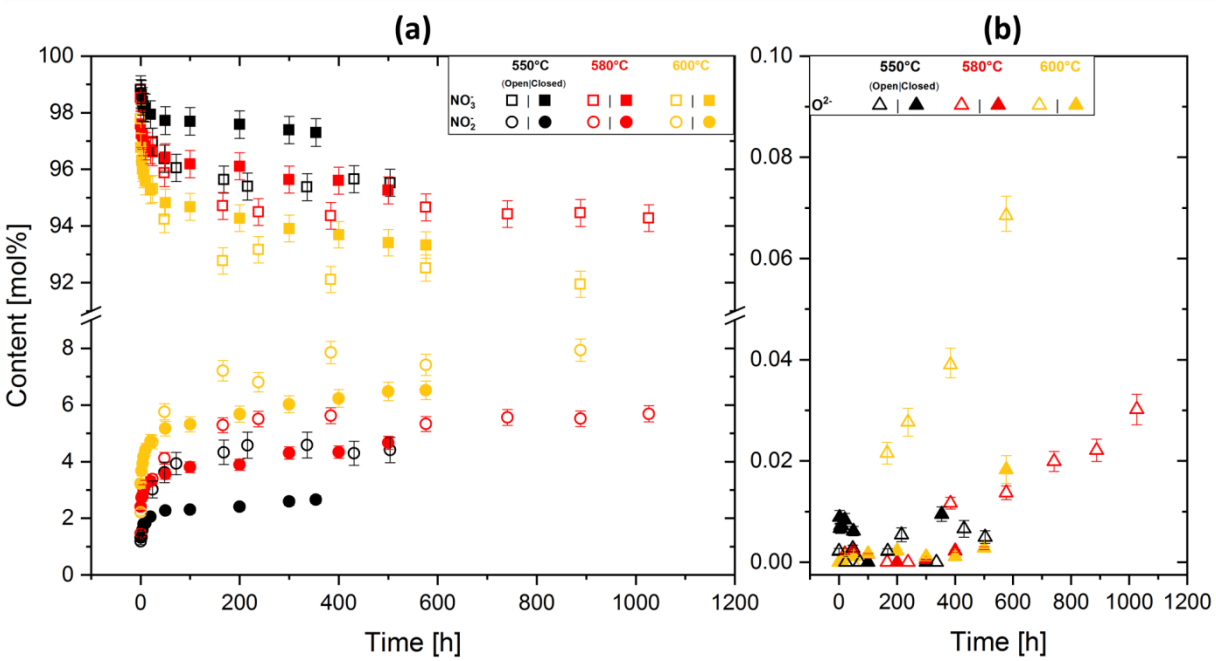

Figure 6 Nitrate and nitrite content in Solar Salt stored in open atmosphere (open symbols) and closed atmosphere (closed symbols). In the *open* configuration the salts were purged with 0.2 atm O_2 in N_2. In the *closed* systems the salts were purged with the same gas at the same flow rate during heating until the salt reached the intended temperature where the system was sealed in terms of salt and gas atmosphere.

The experimental procedures were expanded towards higher temperatures where oxide ion formation is typically enhanced in Solar Salt and it is therefore not considered stable. The molten salt chemistry acquired at 580 °C and 600 °C is shown in Figure 6 including the data already shown in Figure 5 and the molten salt chemistry from classical open atmosphere in Figure 2. It is immediately obvious that the nitrate decomposition and nitrite formation is substantially suppressed in experiments conducted in the closed setup, compared to the open setup. For example the nitrite content in Solar Salt stored at 580 °C in a closed system (95.5 mol%) is equal to that of Solar Salt stored in an open atmosphere at 560 °C. At 600 °C the trends are similar with nitrite contents of 8 mol% in the open system reducing to 6.5 mol% in the closed setup. Nonetheless, when looking at the nitrate and nitrite levels more carefully, they are not in perfect steady state, especially at 580 °C and 600 °C. It is reasonable to assume that this is due to the constant leakage of product gases which affects the chemical equilibrium in the closed vessel. Our expectation is that the steady state can be reached in case the system is sealed hermetically with no pressure loss over time, but elucidation of this hypothesis will hardly be possible since leak-free sealing is not easily reached. The most important

result however, is that the formation of oxide ion species is significantly reduced as shown in Figure 6(b). At 600 °C the oxide contents in the open system are at 0.075 mol% while they are below 0.02 mol% in the closed setup. The same trends are observed for 580 °C, where no measurable oxide ion contents are found (<0.003 mol%) in the molten salt stored in closed configuration, whatsoever, while the oxide ion content steadily increases in the open configuration (0.03 mol% after 1000 h). Overall this indicates that the concentration of corrosive oxide ions is reduced by about 80 % at 580 °C, and 75 % at 600 °C, respectively. The suppressed nitrite formation in the closed system is most likely due to the substantial increase of P_{O_2} during equilibration of the system. The fraction of oxygen (x_{O_2}) and thus the partial pressure during equilibration can be calculated from the change in nitrite content according to Eq. 3.

$$\boldsymbol{x_{O_2}} = \frac{\overbrace{\mathbf{0.5} \cdot (\boldsymbol{x_{NO_2^-,t}} - \boldsymbol{x_{NO_2^-,t=0h}}) \cdot \frac{\boldsymbol{m_{salt}}}{\boldsymbol{M_{salt}}}}^{=evolved\ O_2\ content} + \overbrace{(\boldsymbol{x_{O_2,t=0h}} \cdot \boldsymbol{n_{air,t=0h}})}^{O_2\ content\ at\ t=0h}}{\boldsymbol{n_{air,t=0h}} + \underbrace{\mathbf{0.5} \cdot (\boldsymbol{x_{NO_2^-,t}} - \boldsymbol{x_{NO_2^-,t=0h}}) \cdot \frac{\boldsymbol{m_{salt}}}{\boldsymbol{M_{salt}}}}_{=evolved\ O_2\ content}} \qquad 3$$

Where x_{O_2} is the molar fraction of gaseous O_2, m_{salt} and M_{salt} are the mass and molar mass of Solar Salt respectively, $\boldsymbol{n_{air,t=0h}}$ is the molar content of air at $t = 0h$ derived from the ideal gas law and $\boldsymbol{x_{NO_2^-,t}}$ and $\boldsymbol{x_{NO_2^-,t=0h}}$ are the molar nitrite contents after time t and the starting time $t = 0h$, respectively. When closing the system the oxygen fraction in the gas x_{O_2} is 20 % and thus P_{O_2} is 0.2 atm. The gaseous oxygen released after nitrate-nitrite equilibration (when reaching maximum pressure) adds up to the total fraction of O_2 and our calculations indicate that x_{O_2} after 50 h is significantly higher compared to the start of the experiment. At 550 °C, 580 °C, and 600 °C in the closed system (Fig. 6), the oxygen fraction in the gas was calculated to be 52 %, 51 %, and 49 %, respectively (considering that pressure losses are negligible in that time frame). This is directly convertible to the P_{O_2} which accordingly was 0.84 atm, 0.83 atm, and 0.76 atm. This higher P_{O_2} is ultimately the reason for the shifting equilibrium, which results in lower nitrite contents and similar conclusions can be drawn for the oxide ion contents linked to NO_x-gas formation reaction in Eq. 2. The suppressed decomposition reactions can in turn be interpreted as higher thermal stability of Solar Salt which can effectively push operating temperatures well above

580 °C, or even 600 °C without the excessive degradation detected in the open systems.

3.5. Applicability and Future Prospects

The vast interest in enhanced temperatures in the CSP sector has resulted in R&D towards new storage materials such as carbonate and chloride salts. Undoubtedly, the application temperatures of both classes (>700 °C) are far above the temperatures at which nitrates were tested isothermally so far. The downside of this development certainly is the need for advanced power cycles based on media other than steam, such as supercritical CO_2. Although the advances are promising, they yet appear to be somewhat far from industrial implementation on a significant (e.g. 100 MW-) scale. Sticking to available and already implemented nitrate salts could be beneficial from multiple perspectives. First and foremost, if the salt temperature in the hot tank is increased by only a few ten degrees, modern supercritical steam turbines with steam temperatures of 620 °C - 650 °C could be attached which have higher efficiency than those used in state-of-the-art CSP plants. Even more so, existing coal fired power plants could be upgraded to storage power plants by implementing salt based storage systems with extended hot tank temperatures. Our research indicates that the absolute temperature limit of Solar Salt has not been reached yet. By enriching the gas atmosphere with nitrous gases and/or oxygen, one could not only increase the salt temperature, but by closing it one could avoid the release of harmful gases during operation. Still, effort has to be put into understanding the required partial pressures of reactive gases and the acceptable overpressure in the tanks and the attached gas system. Certainly, one will have to reduce overpressures in the tank to a minimum to be able to make use of state-of-the-art, non-pressurized tank designs. All efforts immediately improve the ecologic footprint, enhance the storage capacity (due to the higher ΔT) and allow TES systems to tap into new markets.

4. Conclusions

The work presented investigates the chemistry of Solar Salt at different temperatures and varying oxygen partial pressures and compares open and closed configurations in terms of thermal stability of the molten salt. The complementary use of in-situ sample extraction from batches of 100 g of Solar Salt with profound post-analysis methods was realized for the first time in this study. This entirely novel technique is

the key for the assessment of the molten salt chemistry under closed atmospheres. Experiments in open configuration demonstrated that the nitrite concentrations in equilibrium increase with increasing temperature and decreasing oxygen partial pressure. In closed configuration the 16 nitrite content can be reduced by 40 %, 20 % and 18 % at 550 °C, 580 °C and 600 °C, respectively. The reduced nitrate decomposition can be traced back to the fact that oxygen gas accumulates in the sealed gas phase (e.g. up to P_{O_2} ~0.5 atm), thereby shifting the equilibrium to the nitrate side. Even more so, the quantity of corrosive oxide ion species is reduced significantly by 80 % and 75 % at 580 °C and 600 °C, respectively, thereby increasing the potential life-time of structural materials. The mechanism likely involves the accumulation of nitrous gases on top of the melt but the exact type of gas species and their concentration have to be confirmed in future studies. Consequently, the molten salts thermal properties in the closed system can be considered stable even at temperatures of 600 °C. These findings constitute a major advance in the design and engineering of next generation TES systems based on molten nitrate salts.

5. Acknowledgements

The authors thank the German Federal Ministry for Economic Affairs and Energy for the financial support given to this work in the MS-STORE project (Contract No. 0325497 A). The authors thank Jochen Forstner for support in chemical analysis and data evaluation. We also thank Prof. Andre Thess for the fruitful discussions during writing of the abstract.

6. Author contributions

A.B., T.B., and V.S. conceived and designed the research. M.B. engineered and built the autoclave test rig as well as the autosampler and performed all experiments. J.F. carried out molten salt analysis by ion chromatography and acid-base titration (acknowledged). A.B. analyzed the data sets. All authors contributed to writing the manuscript.

7. Supporting information

7.1. Description of the autoclave test rig and the autosampler

The isothermal test rig, but more particularly the autosampler are described in more detailed fashion hereafter. The autosampler replaces the manual procedure of sample extraction in the normal test rig configuration, with the heart of it being a 3D-printed, Inconel stand pipe that reaches into the alumina crucible containing the molten salt. The stand pipe has an inner diameter of 1 mm and is heated with compressed (electrically heated) air just before and over the short duration of sample extraction, to avoid solidification of the molten salt in the stand pipe during the extraction process.

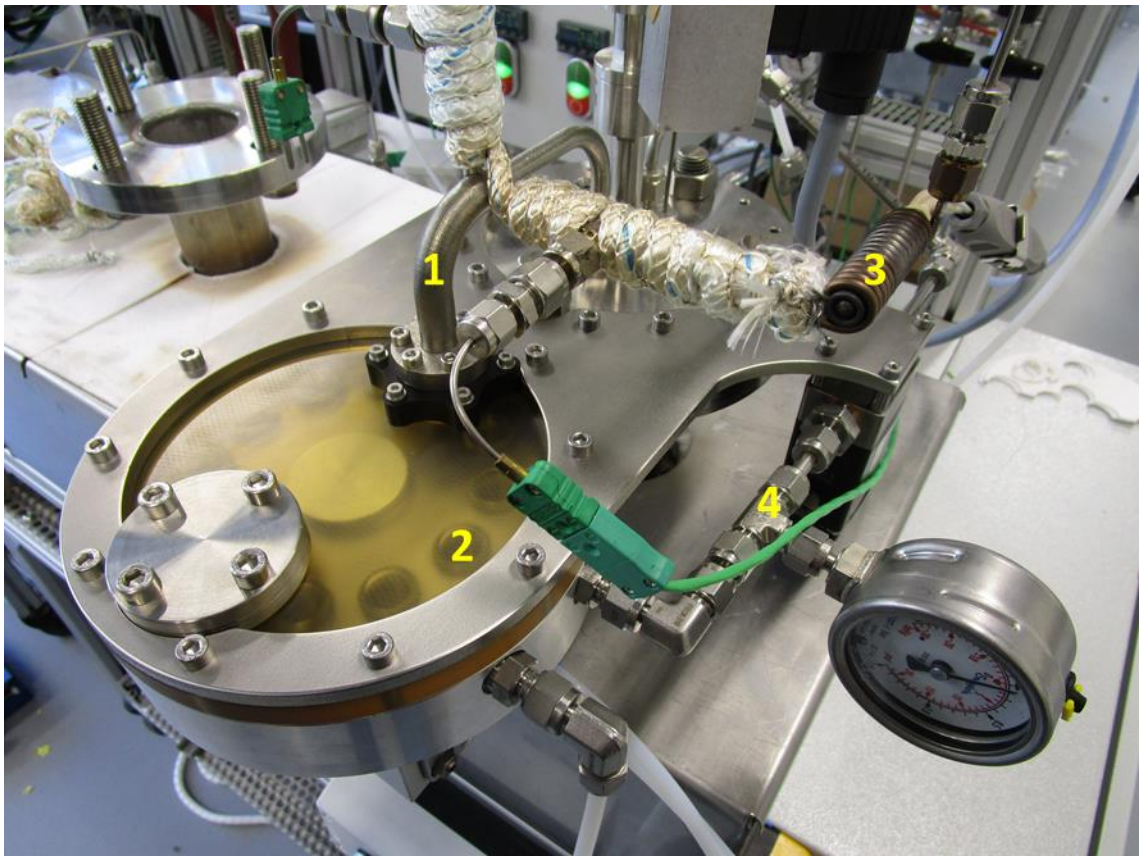

Figure 7 Image of the autosampler attached to the autoclave test rig with the stand pipe (1) used for extraction of molten salt sample from the test rig into one of the 12 sample containers (2), which can be moved pneumatically. The stand pipe is heated with air, heated by a conductive coil (3). The gas system of the autosampler and test rig are connected by a pipe (4) and a complex valve and pressure control system

The autosampler can be regarded a sealed system whose gas atmosphere is connected to that of the autosampler by a complex valve system. It can be explained by looking at Figure 7 more carefully hereafter. during sample extraction the valve between both gas atmospheres (4) is closed and an underpressure is applied in the autosampler (2), leading to the flow of molten salt from the test rig across the stand

pipe (1) into the sample containers of the autosampler. The sealing is achieved by a polysulphone cover, which is the yellowish polymer plate in Figure 7. After setting up the whole system for an experiment, the Solar Salt undergoes a pre-melting step by heating to 300 °C. After reaching this temperature, a pressure test is performed by applying an overpressure of 1 bar (synthetic air), closing the system and measuring the pressure (loss) over time for at least 1 h. After completing the pressure test, the Solar Salt is heated to the intended operation temperature and the system is sealed just when this temperature (e.g. 600 °C) is reached (measured by a thermocouple in the molten salt).

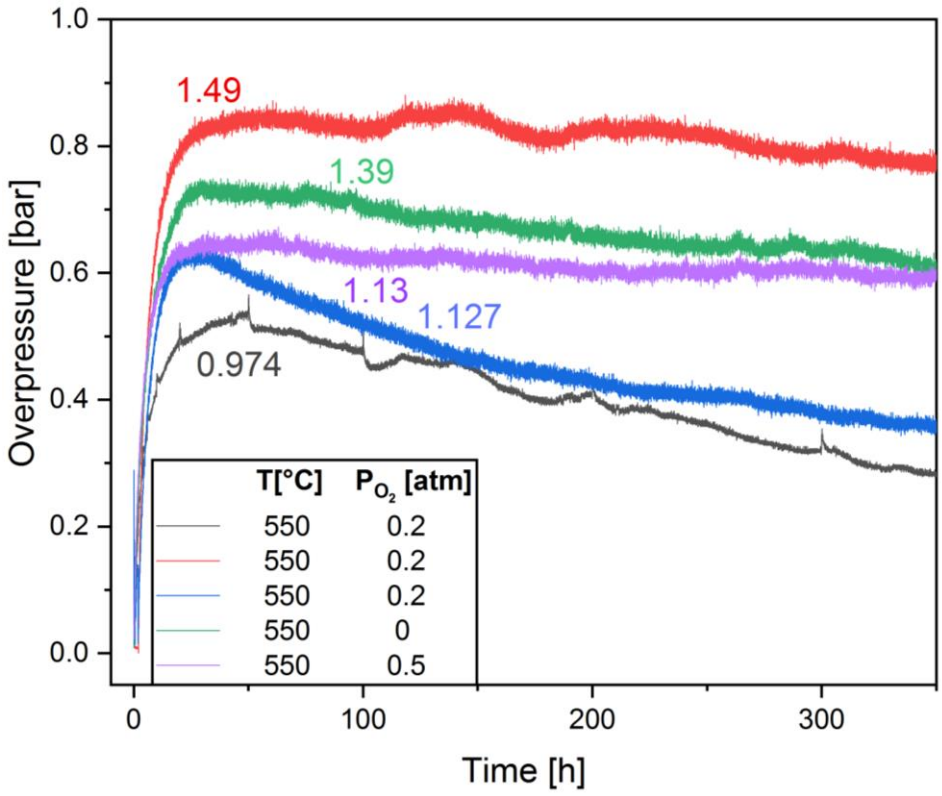

Figure 8 Pressure dataof different experiments with Solar Salt in a system sealed after reaching 550 °C under different (starting) P_{O_2}. Colored designations indicate the change in nitrite content $x_{NO_2^-,max} - x_{NO_2^-,t=0h}$ for the respectively colored pressure curve.

The pressure increase in the system, measured after closing it, was assumed to flow the ideal gas law and thus we assumed that pressure only depends on the change in the number of gas molecules, assuming a constant volume and temperature. We used the following equation for simplicity

$$\Delta P = \frac{\Delta n \cdot R \cdot T_{gas}}{V_{gas}} \qquad 4$$

where ΔP is the change in pressure (overpressure), R is the gas constant, T_{gas} is the temperature, and V_{gas} is the volume of the gas, and Δn is the change of the number of gas particles. Therein, the volume of the gas was derived from the total volume of the closed setup (measured at room temperature) minus the volume of the melt, the latter being calculated from temperature dependent density data (see ref. [7] and literature cited therein). The change in the number of (gas) particles is represented by the (time dependent) quantity of gaseous oxygen $n_{O_2,t}$ evolved during nitrate-nitrite equilibration according to.

$$\boldsymbol{\Delta n = n_{O_2,t}} \quad 5$$

The quantity of evolved oxygen can be calculated, from the change in molar nitrite content according to

$$\boldsymbol{n_{O_2,t} = 0.5 \cdot \left(x_{NO_2^-,t} - x_{NO_2^-,t=0h}\right) \cdot \frac{m_{salt}}{M_{salt}}} \quad 6$$

where $x_{NO_2^-,t}$ and $x_{NO_2^-,t=0h}$ are the molar nitrite contents after a certain experimental time and at t = 0h, respectively, m_{salt} is the mass of salt in the system and M_{salt} is the molar mass of the molten salt (90.8 g mol^{-1} for Solar Salt). Overall the equation for determination of the overpressure can therefore be gained by implementing Eq. 6 into Eq. 5 and then into Eq. 4.

$$\boldsymbol{T_{gas} = \frac{2 \cdot \Delta P \cdot V_{gas}}{\left(x_{NO_2^-,t} - x_{NO_2^-,t=0h}\right) \cdot \frac{m_{salt}}{M_{salt}} \cdot R}} \quad 7$$

For the experiment shown in Figure 4 these assumptions were finally tested. At first, a gas temperature of 550 °C was assumed and for the known change in nitrite content (from 1.2 mol% to 2.49 mol%) the expected pressure increase was calculated to be ΔP = 3.85 bar which is considerably higher than the experimentally gained pressure increase of 0.85 bar (Figure 4). Reviewing the setup we identified that the gas temperature must be the main parameter controlling the pressure increase. The setup contains a crucible that is cooled at its top to avoid salt creeping and salt condensation in the first place. In turn, the gas temperature will be considerably lower at the top, compared to the molten salt temperature at the (heated) bottom and side walls of the system. Consequently, we reshaped Eq. 8 not to identify the theoretically expected pressure increase, but rather use the *measured*

pressure increase, and the known change in nitrite content to calculate the (average) gas temperature in the system according to Eq. 7. For the experiment in Figure 4 a gas temperature of 190 °C was calculated indicating that in fact the average gas temperature drives the overall pressure build-up in the system.

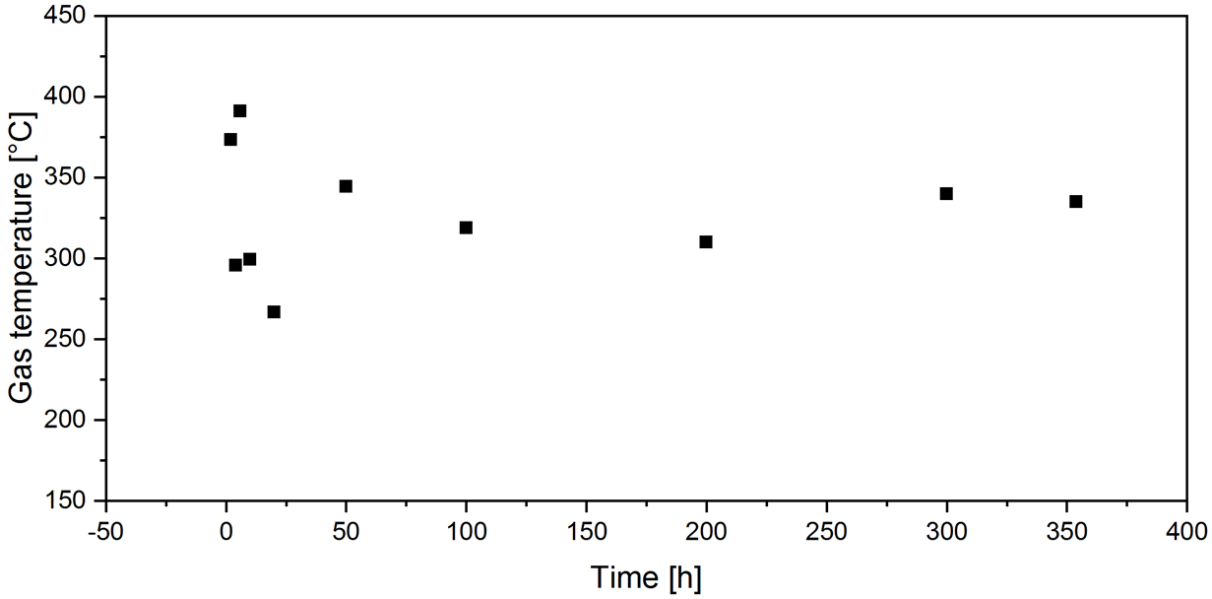

Figure 9 Gas Temperature derived from pressure increase and change in nitrite content according to Eq. 7 for the experiment shown in Figure 5.

To confirm the viability of the approach, the gas temperature was calculated for experiments where the autosampler was used for sample extraction and which was shown earlier in Figure 5. The calculated gas temperatures derived from Eq. 7 for this experiment are shown in Figure 9. The gas temperature seems to be more steady during the end of the experiment, but is more scattering during the first 24 h. The data indicates that there are still some deviations in nominal gas temperature at the start of the experiment, while after equilibration t > 50h the gas temperatures appear to stay constant. Overall, changes in the nitrite content therefore correlate well with recorded changes in pressure and the gas temperature remains the key parameter that affects the pressure in the cell. The large uncertainties at the start of the experiment are most likely due to fact that the melt is further away from chemical equilibrium and therefore changes in the nitrite content are too fast to be recorded accurately. In summary, the ideal gas law can be used to relate changes in pressure with changes in the nitrite content as long as the gas temperature is known.

$$\boldsymbol{\Delta P} = \left[\mathbf{0.5} \cdot \left(\boldsymbol{x}_{\boldsymbol{NO_2^-},t} - \boldsymbol{x}_{\boldsymbol{NO_2^-},t=0h}\right) \cdot \frac{\boldsymbol{m}_{\boldsymbol{salt}}}{\boldsymbol{M}_{\boldsymbol{salt}}}\right] \cdot \frac{\boldsymbol{R} \cdot \boldsymbol{T}_{\boldsymbol{gas}}}{\boldsymbol{V}_{\boldsymbol{gas}}} \qquad 8$$

In Eq. 8 ΔP is the change in pressure (overpressure), R is the gas constant (8.314 J mol^{-1} K^{-1}), V_{gas} is the volume of the gas system, T_{gas} is the temperature, m_{salt} and M_{salt} are the mass and molar mass of the molten salt respectively, and $x_{NO_2^-,t}$ and $x_{NO_2^-,t=0h}$ are the molar nitrite contents after time t and the starting time t = 0h, respectively. Finally, a linear relation between the change in nitrite content and the maximum pressure measured was found when comparing different experiments at 550 °C, which is shown in Figure 10.

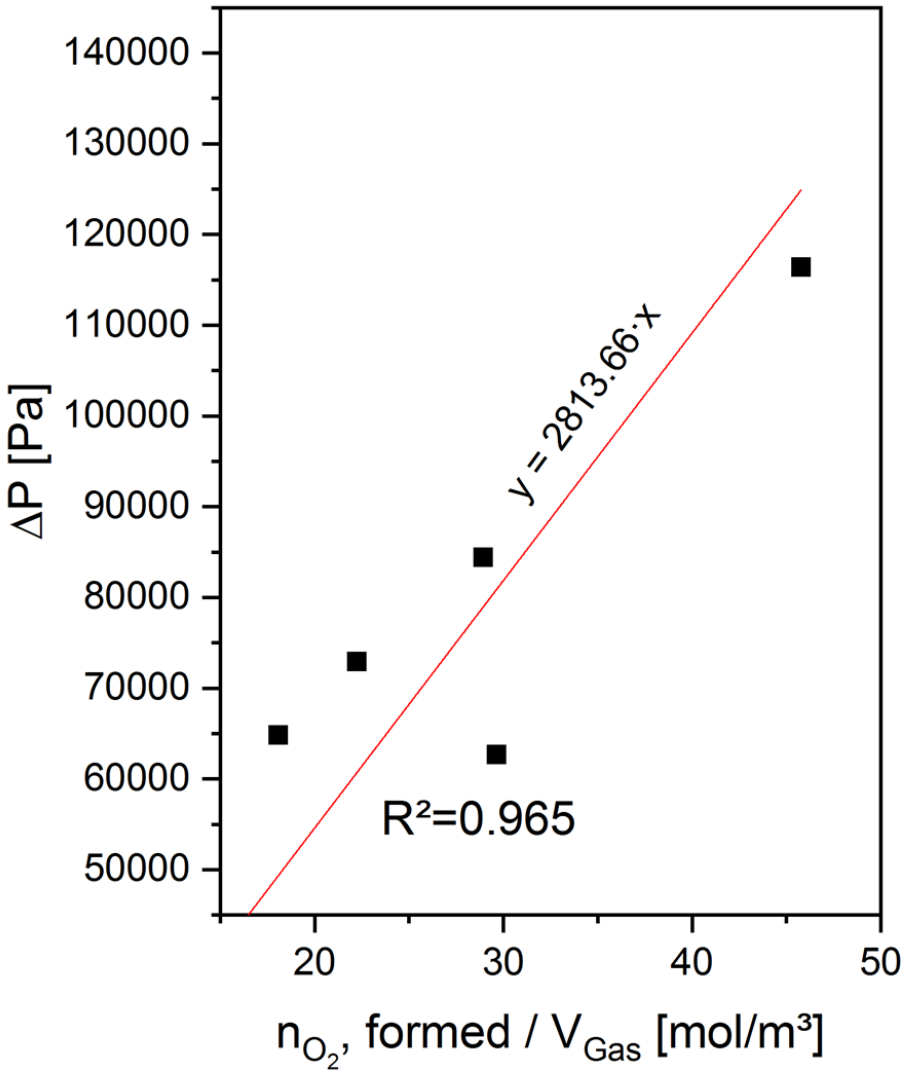

Figure 10 Relation between the maximum pressure during individual experiments and the quantity of O_2 divided by the individual gas volumes in the experiments $\left(\frac{n_{O_2}}{V_{Gas}}\right)$. All experiments were performed with Solar Salt at 550 °C with a starting P_{O_2} of 0.2 atm or 0.5 atm, as indicated in the legend. The figure presents a linear fit function through the data points and the origin.

The values fitted are the maximum pressure during each experiment (typically reached after 25 h to 50 h, see Figure 8) and the change in nitrite content. The nitrite content at the time of pressure maximization can be assumed to remain constant until the end of the experiment. A linear fit function through the origin yields a

correlation coefficient of R^2 = 0.96. From its slope *a* the average gas temperature during these (comparable) experiments can be derived since $a = R \cdot T_{Gas}$, and yields a value of T_{Gas} = 338K. The data proves that the correlations made in Eq. 8 are viable for the correlation of the pressure increase in the cell with the change in nitrite content for systems that feature a similar molten salt temperature and otherwise identical experimental procedures.

References

[1] R. Pitz-Paal, Concentrating solar power: Still small but learning fast, Nature Energy, 2 (2017).
[2] M. Roeb, M. Neises, N. Monnerie, C. Sattler, R. Pitz-Paal, Technologies and trends in solar power and fuels, Energy & Environmental Science, 4 (2011) 2503-2503.
[3] M. Romero, A. Steinfeld, Concentrating solar thermal power and thermochemical fuels, Energy & Environmental Science, 5 (2012) 9234-9234.
[4] R.W. Bradshaw, D.E. Meeker, High-temperature stability of ternary nitrate molten salts for solar thermal energy systems, Solar Energy Materials, 21 (1990) 51-60.
[5] D.A. Nissen, D.E. Meeker, Nitrate-Nitrite Chemistry in NaNO3-KNO3 Melts, Inorganic Chemistry, 22 (1983) 716-721.
[6] T. Bauer, P. Nicole, D. Laing, High temperature molten salts for solar power application, in: Molten Salts Chemistry, Elsevier, 2013, pp. 415-439.
[7] A. Bonk, S. Sau, N. Uranga, M. Herainz, T. Bauer, Advanced heat transfer fluids for direct molten salt line-focusing CSP plants, Progress in Energy and Combustion Science, 67C (2018) 69-87.
[8] M. Mehos, C. Turchi, J. Vidal, M. Wagner, Z. Ma, C. Ho, W. Kolb, C. Andraka, A. Kruizenga, NREL/TP-5500-67464: Concentrating Solar Power - Gen3 Demonstration Roadmap, in, 2017.
[9] A.G. Fernández, J. Gomez-Vidal, E. Oró, A. Kruizenga, A. Solé, L.F. Cabeza, Mainstreaming commercial CSP systems: A technology review, Renewable Energy, 140 (2019) 152-176.
[10] W. Ding, H. Shi, Y. Xiu, A. Bonk, A. Weisenburger, A. Jianu, T. Bauer, Hot corrosion behavior of commercial alloys in thermal energy storage material of molten MgCl2/KCl/NaCl under inert atmosphere, Solar Energy Materials and Solar Cells, 184 (2018) 22-30.
[11] R.W. Bradshaw, Sandia Report SAND2009-8221: Effect of composition on the density of multi-component molten nitrate salts, in, 2009.
[12] T. Bauer, N. Pfleger, N. Breidenbach, M. Eck, D. Laing, S. Kaesche, Material aspects of Solar Salt for sensible heat storage, Applied Energy, 111 (2013) 1114-1119.
[13] R.W. Bradshaw, D.B. Dawson, W. De la Rosa, R. Gilbert, S.H. Goods, et al., SAND2002-0120: Final Test and Evaluation Results from the Solar Two Project, in, 2002.
[14] V.A. Sötz, A. Bonk, J. Forstner, T. Bauer, Microkinetics of the reaction $NO_3^- \rightleftharpoons NO_2^- + 0.5\,O_2$ in molten sodium nitrate and potassium nitrate salt, Thermochimica Acta, 678 (2019).
[15] E.S. Freeman, The Kinetics of the Thermal Decomposition of Sodium Nitrate and of the Reaction between Sodium Nitrite and Oxygen, The Journal of Physical Chemistry, 60 (1956) 1487-1493.
[16] E.S. Freeman, The Kinetics of the Thermal Decomposition of Potassium Nitrate and of the Reaction between Potassium Nitrite and Oxygen 1a, Journal of the American Chemical Society, 79 (1957) 838-842.
[17] E. Desimoni, F. Paniccia, P.G. Zambonin, Solubility and detection (down to 30 p.p.b.) of oxygen in molten alkali nitrates, Journal of Electroanalytical Chemistry and Interfacial Electrochemistry, 38 (1972) 373-379.

[18] J. M. De Jong, G. H. J. Broers, A reversible oxygen electrode in an equimolar KNO3-NaNO3 melt saturated with sodium peroxide - II. A voltammetric study, Electrochimica Acta, 21 (1976) 893-900.
[19] N.P. Siegel, J.B. Cordaro, R.W. Bradshaw, A.M. Kruizenga, Thermophysical Property Measurement of Nitrate Salt Heat Transfer Fluids, in: Proceedings of the ASME 2011 5th International Conference on Energy Sustainability, pp. 54058--54051 - 54058-54058-54058.
[20] S.H. Goods, R.W. Bradshaw, Corrosion of Stainless Steels and Carbon Steel by Molten Mixtures of Commercial Nitrate Salts, Journal of Materials Engineering and Performance, 13 (2004) 78-87.
[21] R.I. Olivares, W. Edwards, LiNO3-NaNO3-KNO3 salt for thermal energy storage: Thermal stability evaluation in different atmospheres, Thermochimica Acta, 560 (2013) 34-42.
[22] A.S. Dorcheh, R.N. Durham, M.C. Galetz, Corrosion behavior of stainless and low-chromium steels and IN625 in molten nitrate salts at 600°C, Solar Energy Materials and Solar Cells, 144 (2016) 109-116.
[23] A. Bonk, D. Rückle, S. Kaesche, M. Braun, T. Bauer, Impact of Solar Salt aging on corrosion of martensitic and austenitic steel for concentrating solar power plants, Solar Energy Materials and Solar Cells, 203 (2019).
[24] A. Bonk, C. Martin, M. Braun, T. Bauer, Material Investigations on the Thermal Stability of Solar Salt and Potential Filler Materials for Molten Salt Storage, AIP Conference Proceedings, 1850 (2017) 080008: 080001-080008-080008.
[25] G.J. Janz, R.P.T. Tomkins, Molten Salts: Volume 5, Part 2. Additional Single and Multi-Component Salt Systems. Electrical Conductance, Density, Viscosity and Surface Tension Data, J. Phys. Chem. Ref. Data, 12 (1983) 591-815.
[26] R.B. Warder, Chemical News, 43 (1881) 228-228.
[27] P. Gauché, J. Rudman, M. Mabaso, W.A. Landman, T.W. von Backström, A.C. Brent, System value and progress of CSP, Solar Energy, 152 (2017) 106-139.
[28] T.R. Tracey, DOE-ET-20314/1-2: Conceptual Design of Advanced Central Receiver Power Systems, in, 1978.